

Hardware in the loop experiments on the interaction between a diesel-mechanical propulsion system and a ventilating propeller

Huijgens, L.J.G.; Vrijdag, A.; Hopman, J.J.

DOI

[10.1080/20464177.2022.2138736](https://doi.org/10.1080/20464177.2022.2138736)

Publication date

2022

Document Version

Final published version

Published in

Journal of Marine Engineering and Technology

Citation (APA)

Huijgens, L. J. G., Vrijdag, A., & Hopman, J. J. (2022). Hardware in the loop experiments on the interaction between a diesel-mechanical propulsion system and a ventilating propeller. *Journal of Marine Engineering and Technology*, 22 (2023)(4), 199-211. <https://doi.org/10.1080/20464177.2022.2138736>

Important note

To cite this publication, please use the final published version (if applicable).
Please check the document version above.

Copyright

Other than for strictly personal use, it is not permitted to download, forward or distribute the text or part of it, without the consent of the author(s) and/or copyright holder(s), unless the work is under an open content license such as Creative Commons.

Takedown policy

Please contact us and provide details if you believe this document breaches copyrights.
We will remove access to the work immediately and investigate your claim.



Hardware in the loop experiments on the interaction between a diesel-mechanical propulsion system and a ventilating propeller

Lode Huijgens, Arthur Vrijdag & Hans Hopman

To cite this article: Lode Huijgens, Arthur Vrijdag & Hans Hopman (2023) Hardware in the loop experiments on the interaction between a diesel-mechanical propulsion system and a ventilating propeller, Journal of Marine Engineering & Technology, 22:4, 199-211, DOI: [10.1080/20464177.2022.2138736](https://doi.org/10.1080/20464177.2022.2138736)

To link to this article: <https://doi.org/10.1080/20464177.2022.2138736>



© 2022 The Author(s). Published by Informa UK Limited, trading as Taylor & Francis Group



Published online: 28 Oct 2022.



Submit your article to this journal [↗](#)



Article views: 527




View related articles [↗](#)



View Crossmark data [↗](#)

Hardware in the loop experiments on the interaction between a diesel-mechanical propulsion system and a ventilating propeller

Lode Huijgens ^a, Arthur Vrijdag ^b and Hans Hopman ^a

^aFaculty of Mechanical, Maritime and Materials Engineering, Delft University of Technology, Delft, the Netherlands; ^bAVR Maritime b.v., Den Haag, the Netherlands

ABSTRACT

The interaction between ship propulsion machinery, propellers and the highly dynamic environment which is the sea is a complex yet highly relevant subject. During a storm, for example, waves and ship motions may cause the propeller to draw air, or ventilate, resulting in rapid changes in propeller thrust and load torque. These fluctuations propagate through the propulsion system, potentially causing excessive loads on propulsion machinery, while also reducing the ship's manoeuvrability. A profound understanding of these complex interactions still lacks. One result of this knowledge gap is the limited acceptance of new technologies for ship propulsion, especially those technologies known to have limited transient capabilities. In this paper, hardware in the loop (HIL) is proposed as a solution to this knowledge gap. Paying specific attention to propeller ventilation, HIL is used to identify new aspects of interaction between engine and propeller, thus demonstrating the added value of HIL for ventilation studies.

ARTICLE HISTORY

Received 8 June 2022
Accepted 16 October 2022

KEYWORDS

Hybrid testing; hardware in the loop; open water test; propeller ventilation; marine propulsion

1. Introduction

In the past decade, ships have become subject to ever stricter requirements. Manoeuvrability, safety and, most notably, environmental impact are under increasing scrutiny. At the same time, cost and profitability remain as important as they have ever been. These increasingly stringent constraints are beginning to pose a problem during the design process. For example, the Energy Efficiency Design Index (EEDI) is progressively limiting installed propulsive power, raising concerns about the ship's manoeuvrability in rough seas (Shigunov and Papanikolaou 2015). At the same time, the manoeuvrability and behaviour of the propulsion system in dynamic environments such as heavy seas is a highly complex subject, leaving considerable uncertainty how both safety and compliance with the EEDI can be achieved. The EEDI is but one challenge in a broader development towards more sustainable shipping. The increasing demands in terms of sustainability will likely require novel propulsion systems to be introduced. Among other solutions, fuel cells are often considered a key technology in this respect. However, as van Biert et al. (2016) noted, the load transient capabilities of certain types of fuel cells may be rather limited. In general, little is known about the performance at full seas of such novel technologies, further adding to the uncertainty regarding the safety and performance of future ships and their propulsion systems.

To address this uncertainty, Vrijdag (2016) and Huijgens et al. (2018) proposed Hardware In the Loop (HIL) propulsion experiments in the model basin. Such experiments combine a hardware hull and propeller with a simulation model of the propulsion system in a single setup, providing insight into the complex interaction between environment, hull, propulsors and machinery. The philosophy behind HIL is to combine complex physics and accurate machinery response in a single experiment. An example of complex physics is the flow around hull and propellers, especially during

manoeuvring and in rough seas. Although the field of computational fluid dynamics (CFD) is rapidly progressing, uncertainty and computational cost still limit the applicability of numerical methods such as CFD to predict manoeuvrability in highly dynamic environments (Carrica et al. 2016). In other words, CFD is currently not able to evaluate the dynamic interaction between propeller and drive with sufficient detail, especially not at longer time scales (Shigunov et al. 2018). At the same time, traditional model basin experiments use a simple propulsion system, resulting in dynamic behaviour that does not correspond to the full scale propulsion system. HIL allows to introduce more realistic propulsion plant behaviour by linking the scale model's propulsion drive to a simulation model of the full scale system. In Figure 1, a schematic representation of such a HIL setup with a free sailing model ship is shown.

HIL experiments with free-sailing model ships were already demonstrated by Tanizawa et al. (2013a, 2013b), who emulated the response of a diesel-mechanical propulsion system in waves. Further steps were taken by Kitagawa et al. (2014, 2015), who introduced real time corrections for scale effects on viscous hull friction and wake fraction, in correspondence with the corrections prescribed by the International Towing Tank Conference ITTC (2011, 2014). Further corrections for rudder effectiveness and propeller torque and thrust in a scale model wake were introduced by Ueno and Tsukada (2015, 2016), with Kitagawa et al. (2019) paying detailed attention to effective propeller inflow in scale model wakes. Similar HIL setups were subsequently used by Ueno et al. (2017), Kitagawa et al. (2018) and Suzuki et al. (2019) to investigate the influence of engine speed governor settings on propulsion plant performance, crash stops and course keeping capabilities. Further HIL experiments with an expanded diesel engine model were presented by Bondarenko and Kitagawa (2021). Noting that viscous scale effects are not the only issue during such HIL experiments,

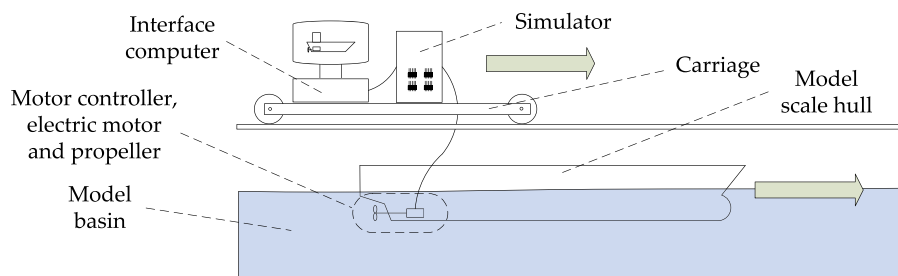


Figure 1. Schematic drawing of a HIL experiment with a free sailing model scale ship. The simulation model, running on the simulator, controls the scale model's electric propulsion motor. The interface computer is used to read out measurements and communicate new settings to the simulator.

Huijgens et al. (2021) paid detailed attention to scale effects inside the propulsion drive. They proposed solutions for distortions of shaft dynamics caused by the electric drive, incorrectly scaled friction and moment of inertia. By subsequent demonstration of these solutions in open water experiments, HIL was validated as an accurate method to emulate the interaction between propulsion machinery and environment.

HIL in the model basin opens up a range of new research directions on the intersection between marine engineering and hydrodynamics. As was mentioned earlier, one could emulate the behaviour of propulsion systems in rough seas, resulting in a better insight into the dynamic loads imposed on machinery in such an environment. Elaborating on this, the aim of this paper is to demonstrate the added value of HIL open water experiments (not in-behind conditions) when investigating the interaction between propulsion machinery and a ventilating propeller. Experiments with free sailing models, as described earlier and shown in Figure 1, require a more advanced setup, while also introducing additional scale effects. Free sailing experiments with ventilation events present an interesting case for future research efforts.

Propeller ventilation occurs if a ship's propeller approaches or pierces the water surface as a result of ship and wave motions, causing air to be drawn between the propeller blades. This not only results in a dynamic loss of propeller thrust, but also introduces potentially problematic fluctuations in propulsion machinery load. As such, propeller ventilation may adversely impact the ship's manoeuvrability and the reliability of the propulsion machinery in adverse weather.

Propeller ventilation has been the subject of hydrodynamic research for decades. However, owing to the complexity of the phenomenon of ventilation, definitive models describing its effect on dynamic propeller performance are yet to be described. As is the case with other hydrodynamic phenomena, early efforts based on first principles and experiments in the model basin have been supplemented by approaches based on CFD and other numerical methods in the course of decades. For example, Swales et al. (1974) conducted experiments on the ventilation of hydrofoils, describing the mechanisms governing ventilation around lift-generating bodies. In a more quantitative approach, Wang et al. (1989) approximated thrust of ventilating propellers based on regression from open water measurements. More recent research efforts on this topic were reported by, among others, Koushan (2007), Califano (2010) and Kozłowska et al. (2020). Apart from model basin experiments, numerical methods have also been used to investigate different aspects of propeller ventilation. Bondarenko and Kashiwagi (2011) used a statistical approach to predict engine speed and load in realistic environments, focussing on speed loss rather than performance on small time scales. Another notable example of a statistical approach on speed loss and power prediction in realistic conditions was presented by Sasaa et al. (2017), who compared numerical simulations with measurement data from actual sea voyages. CFD, too, has been playing an

increasing role in ventilation studies, an early example being the work presented by Califano and Steen (2021).

Yet, most research on propeller ventilation concentrated on the hydrodynamic aspects, neglecting dynamic interaction with the propulsion system as it is present on full scale ships. A notable example is the work by Smogeli (2006), who investigated the interaction between ventilating propellers and propulsion system controllers also in HIL experiments. While also conducting HIL experiments, the setup used by Smogeli (2006) introduced a set of simplifications compared to the setup introduced by Huijgens et al. (2021). For example, Smogeli (2006) did not introduce compensations for friction and moments of inertia. However, as will be shown in this paper, these corrections do introduce additional dynamics, giving a more complete insight into the response of the propulsion system.

A detailed description of the hydrodynamic aspects behind propeller ventilation is outside the scope of this paper. Instead, the aim is to demonstrate the complex yet unexposed interactions between propeller and propulsion machinery during ventilation events using actual HIL measurements, and as such, demonstrate the added value of HIL to investigate the complex phenomenon of propeller ventilation. Although hypotheses are formulated to explain the complex interaction between propeller and machinery, detailed investigation of this subject is reserved for future research.

For the experimental measurements in this paper, the same HIL open water setup is used as described and validated by Huijgens et al. (2021). This setup as well as the approach to conducting HIL measurements will receive detailed attention in Section 2. The measurement data presented in this paper were published in a dedicated folder on the 4TU.ResearchData repository (Huijgens 2020). Every Figure containing measurement data is accompanied by a reference to the relevant data files. Data were recorded using the dSPACE ControlDesk and MATLAB software packages. Data files have the MAT format (.mat). In addition to these data files, the repository contains MATLAB scripts that can assist with visualising the stored measurement data.

2. Method

2.1. Description of HIL open water setup

The experiments described in this paper were conducted with the HIL open water setup introduced by Huijgens et al. (2021); for validation and substantiation of the setup, reference is made to said paper. Figures 2 and 3 show schematic drawings of the full scale propulsion system and the HIL setup considered in this paper. As was explained by Huijgens et al. (2021), HIL experiments are conducted with an open water setup to increase control and reproducibility of the setup and environment. Inevitably, this means that the hydrodynamic interaction between the hull and propeller is not taken into account here. The scope of this paper is limited to demonstrating the interaction between the free surface, propeller and propulsion

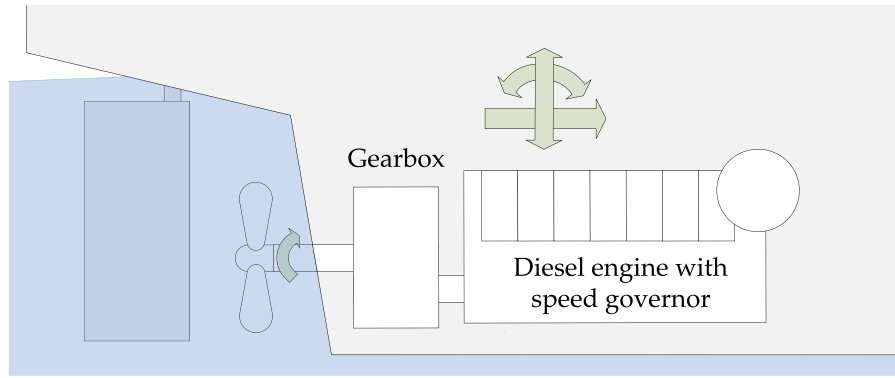


Figure 2. Schematic drawing of the full scale diesel-mechanical propulsion system considered in this paper. This drawing was first published by Huijgens et al. (2021).

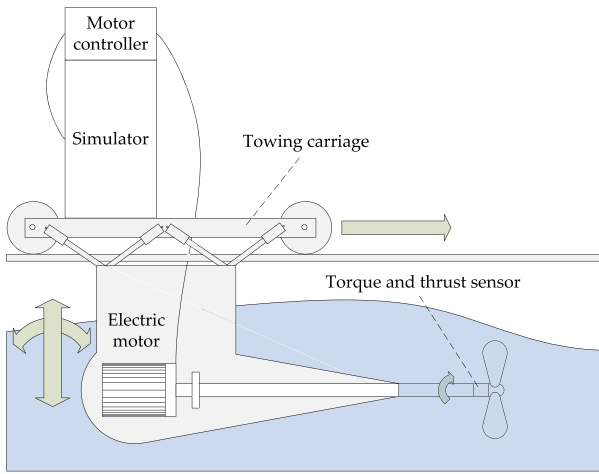


Figure 3. Schematic drawing of the HIL open water setup, used to emulate the diesel-mechanical propulsion system shown in Figure 2. This drawing was first published by Huijgens et al. (2021).

machinery. This is made possible by ensuring correct scaling of polar moment of inertia of the drivetrain as described by Huijgens et al. (2021).

The full scale propulsion system is a constant speed diesel-mechanical drive. The prime mover is a four stroke diesel engine with a nominal brake power of 8336 kW, driving a Wageningen C4-40 propeller with a diameter of 4.2 m through a gearbox. Although this configuration does not exactly match a known full scale equivalent, it combines readily available simulation models and an available, well-documented scale model propeller in a realistic reference case.

The diesel engine runs at a constant speed $n_{e,nom}$. Engine speed is regulated by a PI controller, as is common in modern merchant ships (Bondarenko and Kashiwagi 2010). The gearbox reduces engine speed by a factor of 3.4965, resulting in a propeller shaft speed n_s . The Wageningen C4-40 propeller belongs to a series of controllable pitch propellers developed by Maritiem Research Instituut Nederland (MARIN). The propeller series are described in detail by Dang et al. (2013). The propeller used here has a design P/D ratio of 1.0. The actual P/D ratio is fixed at 1.3 throughout the experiments, which means that the C4-40 is essentially used as a fixed pitch propeller here. If one were to scale down this diesel-mechanical system while avoiding scale effects, one would obtain the *ideal scale model*. This ideal scale model would be dynamically similar to the full scale propulsion system, and is therefore considered as the reference case here. The main parameters of the full scale propulsion system and the corresponding ideal scale model are given in Table 1. For a detailed

Table 1. Main parameters and equilibrium values of the full scale (FS) and ideal model scale (id. MS) propulsion systems.

	Symbol	Unit	FS	id. MS
Equilibrium eng. power	$P_{b,0}$	[W]	6926E3	285.5
Equilibrium eng. torque	$M_{b,0}$	[Nm]	132.3E3	1.289
Equilibrium eng. speed	$n_{e,0}$	[rpm]	500	2115
Gearbox reduction	i_{gb}	[-]	3.4965	3.4965
Eq. prop. torque	$M_{prop,hydro,0}$	[Nm]	462.5E3	4.505
Eq. prop. thrust	$T_{prop,0}$	[N]	572.8E3	99.87
Eq. prop. speed	$n_{s,0}$	[rpm]	143	605
Mech. inertia	I_{mech}	[kgm ²]	54.58E3	0.02970
Added inertia	I_{H2O}	[kgm ²]	6.76E3	0.00368
Prop. P/D ratio	P/D	[-]	1.3	1.3
Prop. diameter	D	[m]	4.199	0.2346
Prop. advance speed	v_a	[m/s]	7.33	1.73
Ship speed	v_s	[m/s]	9.77	2.31

Notes: Geometric scale factor λ equals 17.9; time is scaled according to Froude similarity. The propeller is a Wageningen C4-40 with a design P/D ratio of 1.0. Equilibrium values are given in calm water, without ship motions and propeller ventilation. This Table was first published by Huijgens et al. (2021).

account on the layout of the propulsion plant and the corresponding simulation model, reference is made to Huijgens et al. (2021).

Ideally, the HIL open water setup should perfectly emulate the full scale propulsion system at model scale. In other words, it should be dynamically similar to the ideal scale model. However, Figures 2 and 3 show that the HIL setup introduces a number of components which are different or not present in the actual full scale propulsion system (or in the ideal scale model). These components introduce additional, unwanted dynamic behaviour. Huijgens et al. (2021) and Huijgens (2021) describe the resulting distortions of shaft dynamics – also referred to as scale effects – while also introducing methods to correct for these distortions. Said works contain a detailed comparison of simulated and measured shaft dynamics, indicating that the HIL setup shown in Figure 3 can accurately emulate shaft dynamics of the diesel-mechanical propulsion system represented by Figure 2. Distortions of shaft dynamics and mitigating actions are therefore not further discussed here.

Still, before proceeding to HIL measurements with a ventilating propeller, some additional measurements and simulations are presented in Figures 4 through 6, confirming that the HIL setup can accurately emulate shaft dynamics. These measurements concentrate on the effect of incorrectly scaled moment of inertia on shaft dynamics, as this has proven to be a particularly complex issue to resolve (Huijgens et al. 2021). The moments of inertia of the ideal scale model and practical scale model are given in Table 2.

Figure 4 allows to draw two conclusions. First, the non-linear description of the practical scale model or HIL setup, as it was derived

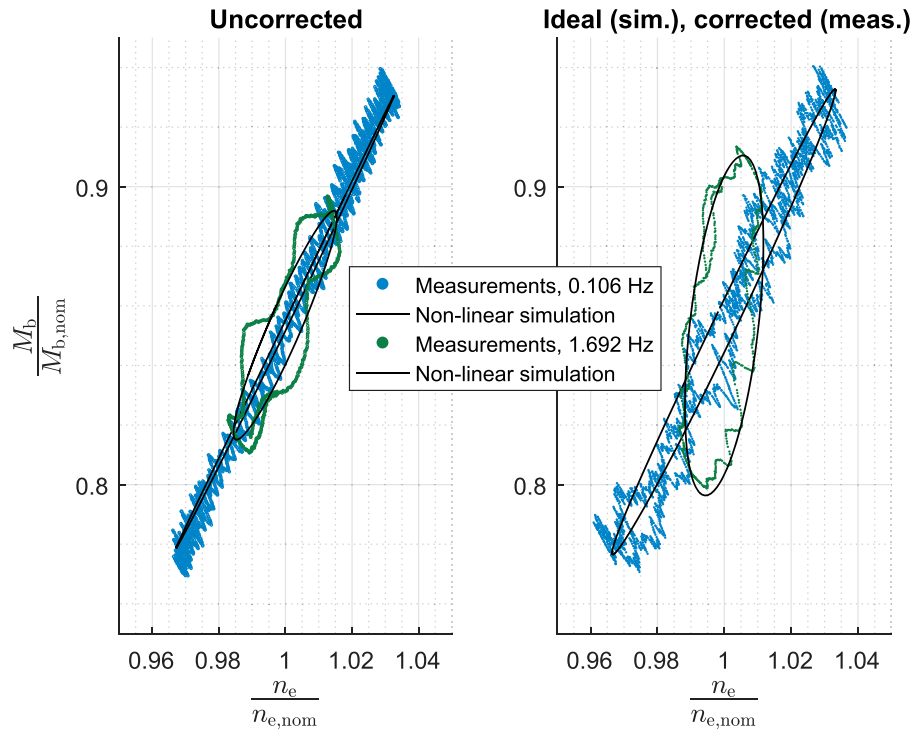


Figure 4. Normalised engine torque and speed during HIL experiments, with and without correction for scale effects on moment of inertia. The speed setting was varied with two different frequencies. For comparison, simulated operating ellipses of the ideal and practical uncorrected scale model are shown as well. These plots are based on the data in *exp_216.mat*, *exp_218.mat* (without inertia correction) and *exp_212.mat*, *exp_214.mat* (with inertia correction), stored in the measurement data repository (Huijgens 2020).

Table 2. Moments of inertia of the ideal and practical scale model propulsion systems.

	Symbol	Unit	Ideal	Practical
Drive moment of inertia	I_d	[kgm ²]	0.02780	0.00226
Prop. moment of inertia	I_{prop}	[kgm ²]	0.00190	0.00064
Mech. moment of inertia	I_{mech}	[kgm ²]	0.02970	0.00290
Added inertia	I_{H_2O}	[kgm ²]	0.00368	0.00368
Total moment of inertia	I_{tot}	[kgm ²]	0.03338	0.00658

Notes: These values correspond to the downscaled diesel-mechanical propulsion system and the actual HIL setup used to emulate the ideal propulsion system. The moment of inertia of the HIL setup is considerably smaller because of lighter propeller material, a more compact propulsion motor and the absence of gear reduction. Added inertia I_{H_2O} is estimated according to Burrill and Robson (1962). This Table was first published by Huijgens et al. (2021).

by Huijgens et al. (2021), is accurate for the response on sinusoidal fluctuations of set shaft speed. At the same time, this proves that the non-linear description of the ideal scale model is valid, too, as the ideal scale model is in fact a simpler version of the practical scale model. Second, the response of emulated engine speed on sinusoidal changes in speed setting is indeed as predicted by the (validated) simulation of the ideal scale model, if all proposed corrections are applied. This demonstrates that the HIL setup can accurately emulate the ideal scale model.

Figure 5 allows to draw the same conclusion for emulated engine speed response on waves. Simulations and HIL experiments were conducted in regular waves with significant waves heights and modal frequencies corresponding to Bft 4, Bft 5 and Bft 6 according to Pierson and Moskowitz (1964). The orbital wave motions cause sinusoidal fluctuations of propeller load, which propagate through the propulsion system to the (simulated) diesel engine. Again, simulations of the ideal scale model align well with HIL experiments if the proposed corrections are applied.

To verify that the HIL setup is also able to emulate non-linear dynamics at small time scales, Figure 6 shows the simulated and measured response of drive torque the instant after a considerable step change in engine speed setting. Here, too, the measured response with corrections coincides well with the simulated response of the ideal scale model. In other words, high-frequent non-linear phenomena as they may occur during propeller ventilation events can be accurately emulated, too.

An important topic in the area of propulsion system dynamics is the inertia of the entrained water. For the simulations mentioned in this Section, added inertia I_{H_2O} was determined as proposed by Burrill and Robson (1962). There are several methods to determine added inertia terms, prominent examples being Lewis and Auslaender (1960) and Schwanecke (1963). Another relevant method was presented by Parsons et al. (1980), who conducted measurements to derive added mass matrices for the Wageningen B propeller series – a propeller series comparable to the Wageningen C used here. Even though the validity of these methods are sometimes disputed (Krüger and Abels 2017), they provide a good starting point to estimate added inertia in relatively simple cases such as regular waves. This allows to compare the response of the HIL setup to non-linear simulations in such environments.

For the more complex cases discussed in Section 3, three added mass terms are relevant: axial added mass m_{11} , entrained inertia m_{44} (which equals I_{H_2O}) and axial-rotational coupling term m_{14} . Propeller thrust breakdown and recovery is influenced by terms m_{11} and m_{14} , while torque breakdown and recovery depends on terms m_{44} and m_{14} . As was indicated earlier, Parsons et al. (1980) estimated these coefficients by regression of measurement data. More modern approaches permit purely numerical estimation of these parameters, as demonstrated by Martio et al. (2015) who used URANS, or Li et al. (2018), who used a frequency domain panel method. However, as was discussed in Section 1, modern numerical approaches are subject to uncertainties, too, and are often a compromise between

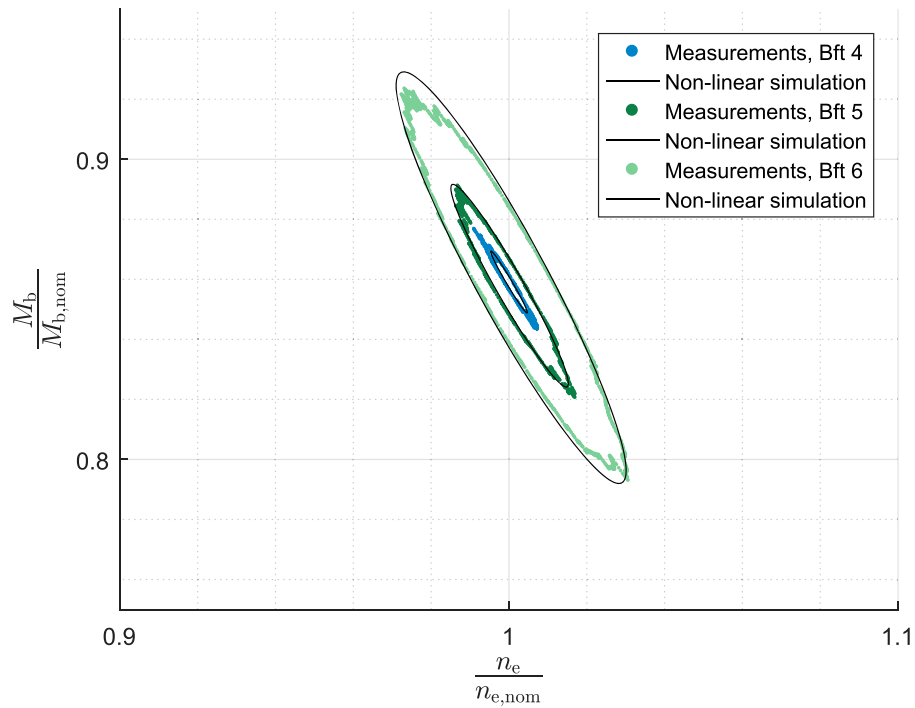


Figure 5. Normalised engine torque and speed during HIL experiments with corrections as proposed by Huijgens et al. (2021) and non-linear simulations of the ideal scale model. Operating ellipses are shown for regular waves with a significant wave height and model frequency according to Bft 4, Bft 5 and Bft 6. The equilibrium values of the simulated ellipses are increased by approximately 4% in order to coincide with the measured equilibrium points. This Figure is based on the data in *exp_234.mat*, *exp_235.mat* and *exp_236.mat*, stored in the measurement data repository (Huijgens 2020).

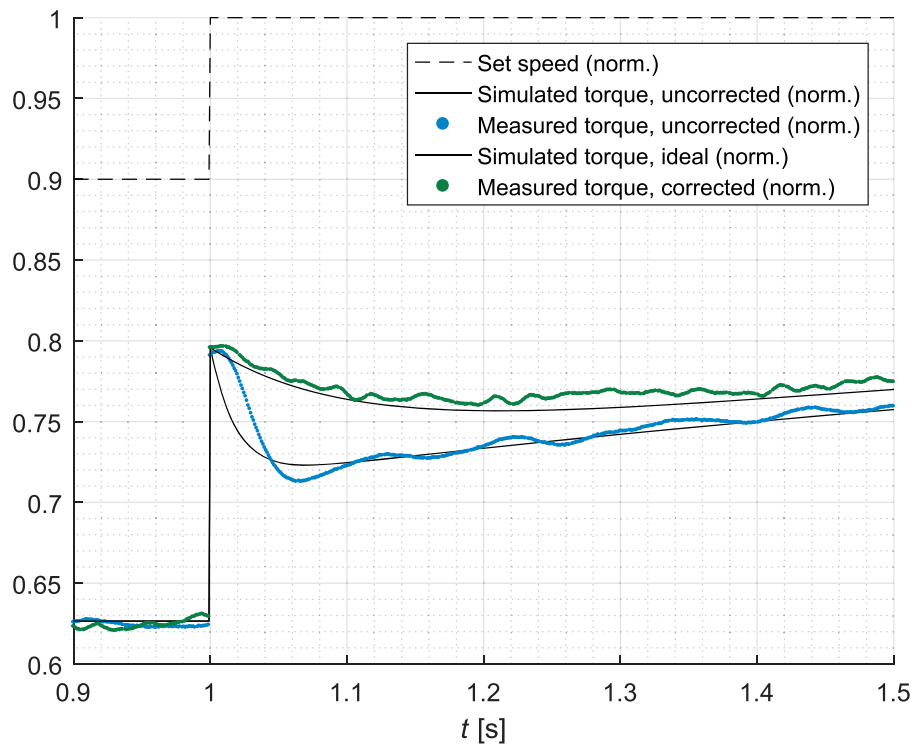


Figure 6. Normalised engine torque response on a step change in speed setting during fully numerical simulations and HIL open water experiments. Speed and torque are normalised with respect to their nominal values. As is the case in Figures 4 and 5, engine torque behaves as predicted by validated simulations. This Figure is based on the data in *exp_220.mat* (without inertia correction) and *exp_219.mat* (with inertia correction), stored in the measurement data repository (Huijgens 2020).

Table 3. Conditions during the HIL experiments with propeller ventilation described in this paper.

	Symbol	Unit	Measured
Eq. propeller torque	$M_{\text{prop,hydro},0}$	[Nm]	4.7
Eq. propeller thrust	$T_{\text{prop},0}$	[N]	102.4
Eq. propeller speed	$n_{s,0}$	[rpm]	605
Propeller advance speed	v_a	[m/s]	1.37
Propeller immersion	h	[m]	0.218
Wave peak frequency	ω_p	[rad/s]	3.3
Wave encounter frequency	ω_E	[rad/s]	5.2
Wave amplitude	A_w	[m]	0.140

Note that equilibrium values are applicable for calm water conditions.

accuracy and acceptable compute-intensity. In this context, it is interesting to note that studies on added mass coefficients for propellers operating in multi-phase flows are exceedingly rare. The use of purely numerical methods to study long term propulsion plant dynamics is therefore limited. A significant advantage of HIL lies in the fact that added mass and all related dynamics around the propeller occur physically, eliminating the need for numerical estimation of added mass coefficients. Considering this, these coefficients are not covered in further detail here.

The results shown in Figures 4, 5 and 6 reaffirm the more detailed analyses conducted by Huijgens et al. (2021) and Huijgens (2021). With the capabilities of the HIL open water setup demonstrated, the added value of HIL for experiments with propeller ventilation can be investigated.

2.2. HIL experiments with propeller ventilation

The added value of HIL to investigate the interaction between propulsion machinery and a ventilating propeller are demonstrated in Section 3. Two distinct comparisons are made. First, open water experiments with a ventilating propeller with and without HIL are compared, illustrating the added value of HIL compared to traditional, constant-speed experiments. Second, measurements with and without correction for the moment of inertia are compared, demonstrating the relevance of this inertia correction. All experiments were conducted under similar conditions, given in Table 3. The wave height and peak frequency corresponds to the (downscaled) significant wave height and modal frequency in Bft 5, as predicted by the Pierson-Moskowitz wave spectrum for fully developed seas (Pierson and Moskowitz 1964).

Experiments were conducted with a propeller which was moved through a towing tank in a fixed, forward direction, meeting head waves generated by a wave maker. Propeller depth was chosen such that the top of the blades pierced the surface in wave troughs. In these conditions, three distinct stages of propeller ventilation were observed, schematically represented in Figure 7. In the first stage, the propeller operates under a wave peak. It is relatively deeply submerged, and interaction with the free surface is negligible. An image still of this stage, captured during an actual ventilation experiment, is shown in Figure 8. As the propeller moves away from the wave peak, the distance from the free surface drops, which means that the pressure gradient between the atmosphere and propeller suction side increases. At a certain point, this pressure gradient becomes large enough to cause deformation of the free surface; this is observed in stage II. Figure 9 shows an image still of this stage. Finally, in stage III, the propeller blade tips pierce the surface. At this point, air is entrained between the propeller blades as can be witnessed from Figure 10. This results in a collapse of propeller torque and thrust. In a real, full scale situation, this limits a ship's speed and manoeuvrability, while also imposing potentially dangerous load fluctuations on the propulsion plant. If the propeller is again submerged to a

sufficient depth for a sufficient amount of time, this air is blown out of the propeller, and torque and thrust are restored. To determine how fast torque and thrust are restored in real, full scale system, HIL is required, as is demonstrated in Section 3.

3. Results and discussion

3.1. Added value of HIL for experiments with propeller ventilation

A first series of experiments with propeller ventilation was conducted with and without emulated diesel-mechanical propulsion system. The propeller was moved through a wave train, with immersion depth of the propeller limited such that the propeller pierces the surface in the troughs of the largest waves. The wave amplitude of the wave train increases and decreases over a period of time, resulting in a dynamic breakdown and recovery of propeller thrust. Conditions during these experiments are given in Table 3.

Figure 11 displays immersion depth, torque and thrust of the propeller measured during these first series of experiments. Here, propeller immersion depth is defined as the distance between the centre of the propeller hub and the free surface. It is measured next to the propeller using a conductivity sensor. The shown 12 second trace can be roughly divided into three phases. In the first phase, wave heights are too small to cause significant ventilation. In this phase, the difference in thrust response between the HIL and constant speed cases – a smaller amplitude of thrust fluctuations and a minor phase lag for the HIL case – can be attributed to the slower response of the emulated ship machinery when HIL is applied. This effect was also reported by Huijgens et al. (2021). In the constant speed case, the propulsion system is not emulated, and speed is controlled more stiffly. This results in smaller speed fluctuations as propeller inflow varies and thus, larger fluctuations of propeller thrust.

0:18.5 marks the approximate beginning of the second phase, in which the propeller starts drawing air. As Figure 9 shows, no vortices occur, while the free surface above the propeller clearly deforms prior to ventilation events. This type of ventilation is referred to as condition III by Kozłowska et al. (2009), and occurs only in case of limited propeller submergence. Indeed, propeller submergence in these experiments is limited to such an extent that the propeller disk pierces the water in the largest wave troughs. After the first ventilation inception, some air remains entrained between the propeller blades for the duration of the second phase; differently put, the propeller does not completely recover from ventilation in between wave troughs until the third phase. In the third phase, which starts from approximately 0:23, entrained air has mostly disappeared, gradually resulting in the same situation as in the first phase.

Experiments at constant propeller speed and HIL experiments both show considerable effects of ventilation on propeller thrust. Between 0:18.5 and 0:23, every wave trough causes air to be drawn by the propeller, resulting in an immediate thrust breakdown for both the constant speed case and HIL case. However, the subsequent

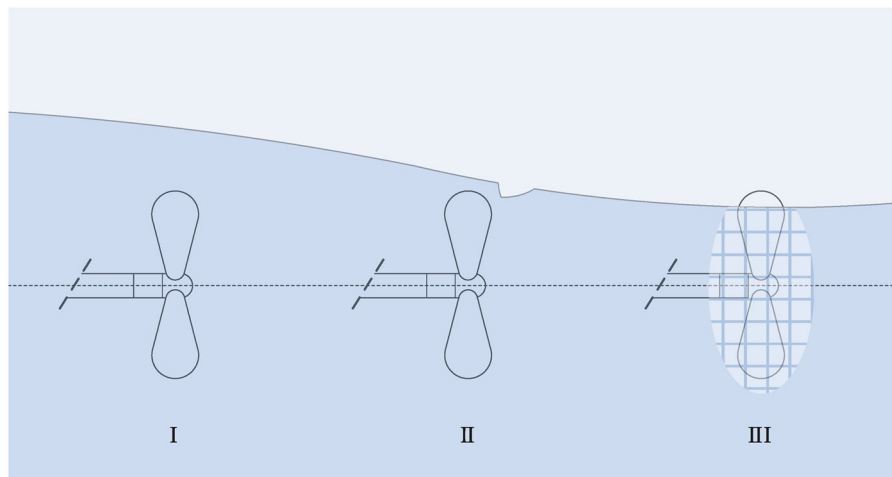


Figure 7. Three stages of propeller ventilation observed during open water experiments with a surface piercing propeller. In stage I, the propeller is fully submerged, and interaction with the free surface is negligible. In stage II, the pressure difference between the atmosphere and propeller suction side causes the free surface to deform. In stage III, the propeller pierces the surface, and air is entrained between the propeller blades.

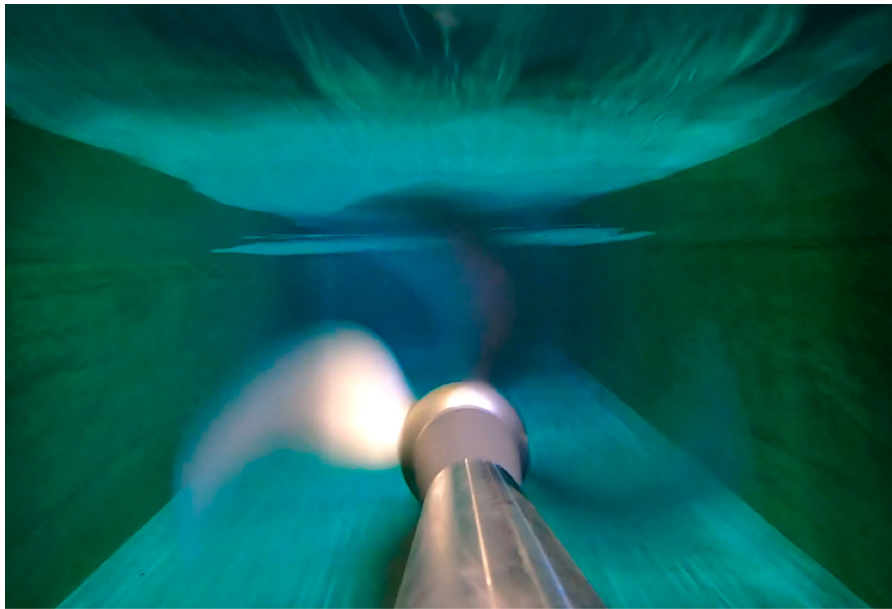


Figure 8. Looking forward from behind the propeller while the propeller is operating under a wave peak. This situation corresponds to stage I in Figure 7.

course of thrust breakdown and recovery is considerably different. The loss in thrust is greater in the case with HIL emulation, at times nearly 20% lower than during the constant speed experiment. In addition, thrust seems to recover after each wave in the constant speed experiment, whereas the HIL experiment shows a more complex, prolonged loss of thrust. This difference is caused by the slow response of the diesel-mechanical propulsion system, which is emulated in the HIL experiment but not in the constant speed experiment. The emulated diesel-mechanical drive introduces a large moment of inertia, while also including an additional PI speed controller. This results in more sluggish response on changes of shaft speed, and therefore, a reduced ability to maintain thrust in a rapidly fluctuating environment. The constant speed experiment, on the other hand, only contains a very stiffly controlled electric motor with a relatively low moment of inertia. Being able to respond faster, it avoids the large thrust losses associated with the diesel-mechanical plant. Thus, the constant speed experiment fails to accurately assess dynamic thrust loss as it occurs in a real, full scale situation.

Zhang et al. (2021) conducted experiments with a ventilating propeller and rigid speed control, noting that thrust is restored approximately 5 propeller rotations after full submergence following a ventilation event. For the experiments in this paper, 5 propeller rotations correspond to approximately one half second. Keeping this in mind, the measurements conducted without HIL shown in Figure 11 seem to confirm the observation by Zhang et al. (2021). The last wave trough causing air entrainment occurs shortly after 0:22; for the constant speed case, thrust again follows an undisturbed, sinusoidal path before 0:23. For the HIL case, however, thrust is not restored until several seconds later, around 0:25.

In addition to the fluctuations caused by the interaction between the propulsion system and its environment, conspicuous fluctuations with a frequency of approximately 10 Hz can be observed. 10 Hz is also the frequency of shaft rotations, indicating that this fluctuation stems from a small eccentricity in the shaft. This issue is discussed in more detail in Huijgens (2021).

These measurements show that propulsion plant dynamics indeed have a profound impact on thrust loss during ventilation

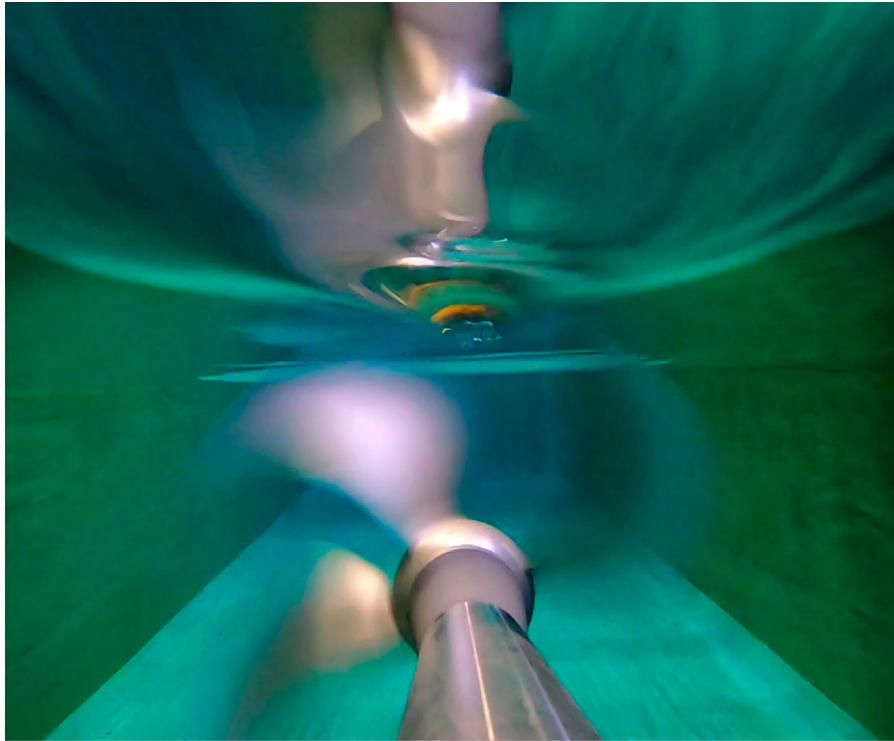


Figure 9. Looking forward from behind the propeller, the instant before ventilation inception. The pressure at the suction side of the propeller is significantly lower than the atmospheric pressure. This causes air to be drawn towards the propeller, as witnessed by the local deformation of the free surface in front of the propeller. This situation corresponds to stage II in Figure 7.

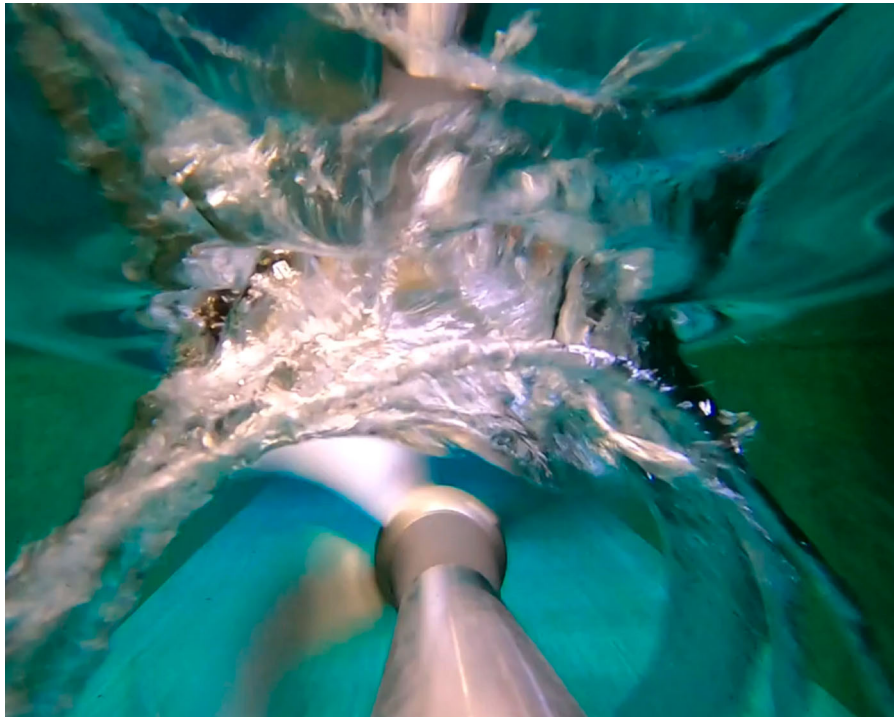


Figure 10. Looking forward from behind the propeller while the propeller pierces the surface. Water is entrained between the propeller blades, causing propeller torque and thrust to collapse. This situation corresponds to stage III in Figure 7.

events as they occur, for example, in rough seas. This was noted before, and some research on ventilation did take into account propulsion system dynamics. For example, Smogeli (2006) investigated ventilation while also considering, to some extent, the dynamic properties of the propulsion drive and control system. Noting scale

effects on moment of inertia, Smogeli (2006) also considered an inertia correction. However, no such correction was eventually applied, as it was concluded that the influence of inertia on system response is negligible. This is an interesting observation, as it seems to contradict simulations and measurements reported by Huijgens et al. (2021).

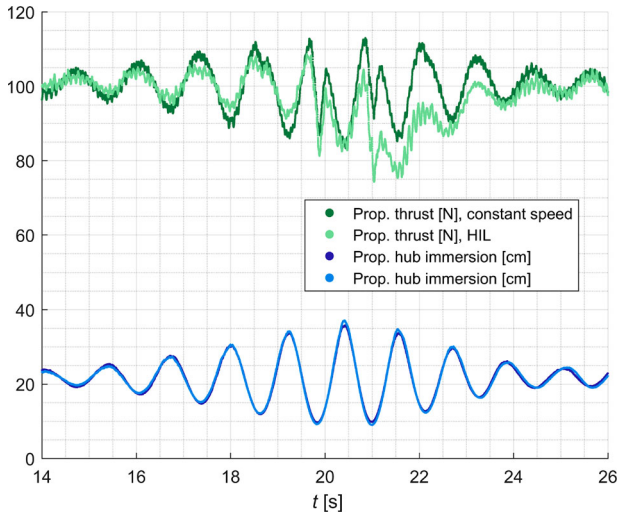


Figure 11. Time trace of measured propeller thrust, with constant propeller speed (*constant speed*) and with emulated diesel-mechanical propulsion system (*HIL*). Time is expressed at model scale, with time scaled according to Froude's law. Measured thrust is filtered by a low-pass filter with a time constant of 0.0159 s. The conditions during these experiments are given in Table 3. This Figure is based on the data in *exp_251.mat* (*constant speed*) and *exp_250.mat* (*HIL*), stored in the measurement data repository (Huijgens 2020).

As such, this observation presents a good occasion to pinpoint the added value of the corrections proposed by Huijgens et al. (2021). In Section 3.2, the influence of the inertia correction on the emulated dynamics is investigated in particular in a second series of HIL experiments with propeller ventilation.

3.2. Added value of inertia correction for experiments with propeller ventilation

To demonstrate the added value of the inertia correction for HIL tests in the ship model basin, experiments were conducted under the conditions described by Table 3, with and without inertia correction. Figure 12 shows propeller torque and thrust measured during these experiments. Under the given conditions, the influence of moment of inertia on propeller performance appears to be negligible: the traces for the corrected and uncorrected cases largely overlap. This seems to confirm the observations by Smogeli (2006).

At 0:52, the propeller speed of the setup with inertia correction is approximately 5% lower than for the uncorrected setup; measured propeller torque and thrust, however, are not. This may indicate that during a ventilation event, torque and thrust much more depend on the amount of entrained air during ventilation and the time-averaged torque and thrust – which are identical for the corrected and uncorrected case – rather than propeller speed. Yet, this independency between shaft speed and propeller performance may not hold for all cases; a systematic evaluation could shed more light on this topic.

Contrary to propeller torque and thrust, however, the dynamic response of engine torque and speed does depend on moment of inertia, as appears from Figure 13. During each ventilation event, shaft speed and thus, engine speed rapidly increases as the load partly disappears. At this point, the difference in moment of inertia becomes apparent. As can be seen in Figure 13, the shaft responds more sluggish if the inertia correction is applied – note that the correction virtually increases inertia in this case. The increased sluggishness can be explained by the added, virtual moment of inertia, causing an increased part of the acceleration torque to be virtually absorbed as inertial torque (or released, in case of deceleration). This in turn results in reduced shaft acceleration and deceleration.

This observation leads to the question why the response of engine torque and speed does change if the inertia correction is applied, while such a change is not observed for propeller load torque and thrust. Differently put: why does a changing moment of inertia affect load and drive in a different way? The answer to this question is found by identifying the different components of which measured load torque and emulated engine torque consist. A schematic representation of these torque components is given in Figure 14. Propeller torque, on one hand, is measured right in front of the propeller, as was also shown in Figure 3. Measured propeller torque $M_{\text{prop},m}$ therefore consists of the hydrodynamic load torque of the propeller, $M_{\text{prop,hydro}}$, the inertial torque of the propeller, related to propeller inertia I_{prop} , and the inertial torque of the entrained water, related to entrained inertia $I_{\text{H}_2\text{O}}$. Equation (1) expresses $M_{\text{prop},m}$ in mathematical terms.

$$M_{\text{prop},m} = M_{\text{prop,hydro}} + (I_{\text{prop}} + I_{\text{H}_2\text{O}}) \cdot \frac{d\omega}{dt} \quad (1)$$

Engine torque M_d , on the other hand, includes all torque components in the propulsion system. It consists of the inertial torque of the complete (emulated) propulsion drive, which follows from propulsion drive inertia I_d , on top of the torque components present in the $M_{\text{prop},m}$. Note that friction losses are corrected in the HIL experiments, as was explained by Huijgens et al. (2021), and can therefore be neglected here. Equation (2) expresses M_d in mathematical terms.

$$M_d = M_{\text{prop,hydro}} + (I_d + I_{\text{prop}} + I_{\text{H}_2\text{O}}) \cdot \frac{d\omega}{dt} \quad (2)$$

Compared to measured propeller torque, engine torque thus contains an additional inertia component related to propulsion drive inertia I_d . The fact that the additional inertia, introduced by the numerical inertia correction, is virtually added to I_d , explains why the dynamic response of M_d is affected significantly by this correction. As $M_{\text{prop},m}$ does not contain the I_d term, measured propeller torque is not directly affected by a change in moment of inertia on the drive side, irrespective of whether this change occurs virtually or physically.

With this, an important distinction between propeller load and machinery load becomes apparent. In a dynamic environment, the load torque of the propulsion machinery may fluctuate more than one would expect based on measured propeller load. In addition to propeller torque, drive torque contains inertial components which, depending on machinery, controller settings and environment, may become considerable. Failing to identify these could lead to a significant underestimation of dynamic machinery load.

It should be noted that this de-coupling between propeller and prime mover dynamics may not occur for all propulsion systems. As was shown, the absence of the inertial term I_d in measured propeller torque $M_{\text{prop},m}$ plays a key role. If this term becomes smaller – for example, as a result of a smaller and lighter prime mover –, this effect may become less pronounced. A sensitivity analysis in future work could provide more insight into this topic.

In summary, Figures 12 and 13 show that in the case considered in this paper, the engine responds entirely different on its environment than does the propeller. The response of propeller torque and thrust appears to be mostly independent of shaft speed fluctuations and therefore, parameters such as moment of inertia, at least for the propulsion system considered here. The response of the propulsion machinery, on the other hand, is considerably affected by distorted inertia, as the drive torque contains inertial components that are not present in the propeller load torque. In the case shown in Figure 13, peaks in engine torque are approximately 30% smaller if the inertia correction is applied, while speed peaks are approximately 20%

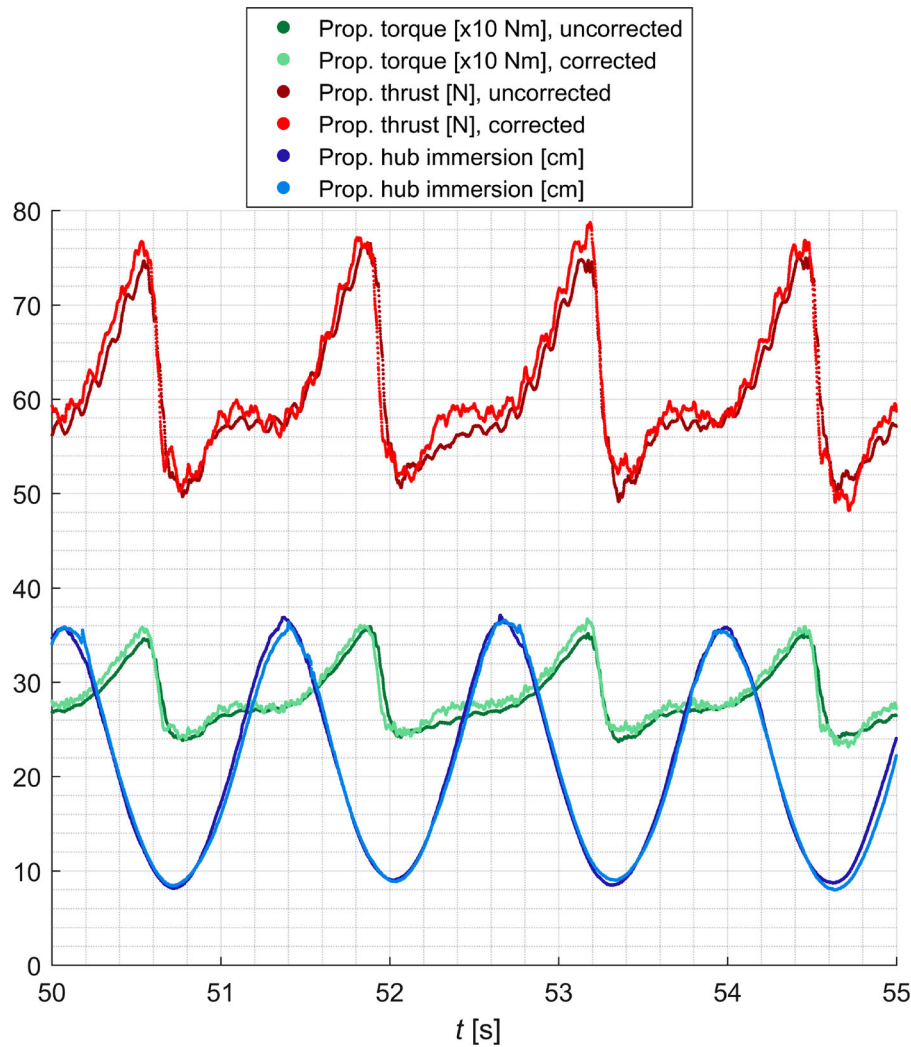


Figure 12. Time trace of measured propeller torque and thrust during HIL experiments with an emulated diesel-mechanical propulsion system, without and with numerical inertia correction. Time is expressed at model scale, with time scaled according to Froude's law. Measured torque and thrust are filtered by a low-pass filter with a time constant of 0.0159 s. The equilibrium immersion depth of the propeller hub equals 0.218 m. The conditions during these experiments are given in Table 3. This Figure is based on the data in *exp_245.mat* (without inertia correction) and *exp_242.mat* (with inertia correction), stored in the measurement data repository (Huijgens 2020).

smaller. Moreover, the behaviour between peaks is entirely different. Notwithstanding reservations regarding scale effects, it is plausible that these effects also occur at full scale given their observed magnitudes during the experiments reported here. These observations allow to formulate conclusions and recommendations, as is done in Section 4.

4. Conclusions and recommendations

The results presented in Section 3 allow to draw three conclusions. First, the measurements and simulations shown in Figures 4, 5 and 6 show that HIL open water experiments can accurately emulate shaft dynamics of the considered propulsion system, also at small time scales. In particular, this means that the complex interaction between ship propulsion systems and ventilating propellers can be accurately emulated using HIL.

Second, it is concluded that HIL is required to make a realistic evaluation of the full scale interaction between propulsion plant and propeller during ventilation events. Figure 11 shows that for the considered case, thrust loss during HIL open water experiments is approximately 10% higher than during traditional, constant speed experiments. In addition, propeller thrust takes longer to recover

from ventilation events in the HIL experiment. These effects can be attributed to the emulated ship propulsion system, which responds significantly slower than the electric drive of the scale model. This difference in predicted thrust loss likely also depends on variables such as the wave encounter frequency and properties of the emulated propulsion system. If these are changed, the difference in predicted thrust loss may become smaller or larger; this dependency was not systematically investigated here. In any case, failing to predict these dynamic interactions may lead to overestimation of propulsive thrust and thus, speed and manoeuvrability in adverse weather, with detrimental consequences for ship designs.

The third conclusion pertains the relevance of the correction for moment of inertia. Interestingly, the inertia of the emulated propulsion system does not seem to be relevant for the dynamic torque and thrust of the propeller. As the propeller starts drawing air, propeller torque and thrust appear to become less dependent on shaft speed. It must be noted that the influence of governor settings and other properties of the propulsion system on propeller performance were not investigated; these may have an important influence that remained unnoticed here. Yet, the moment of inertia did have a profound impact on the shaft speed and torque of the simulated diesel engine. This relation is caused by the additional inertial torque component

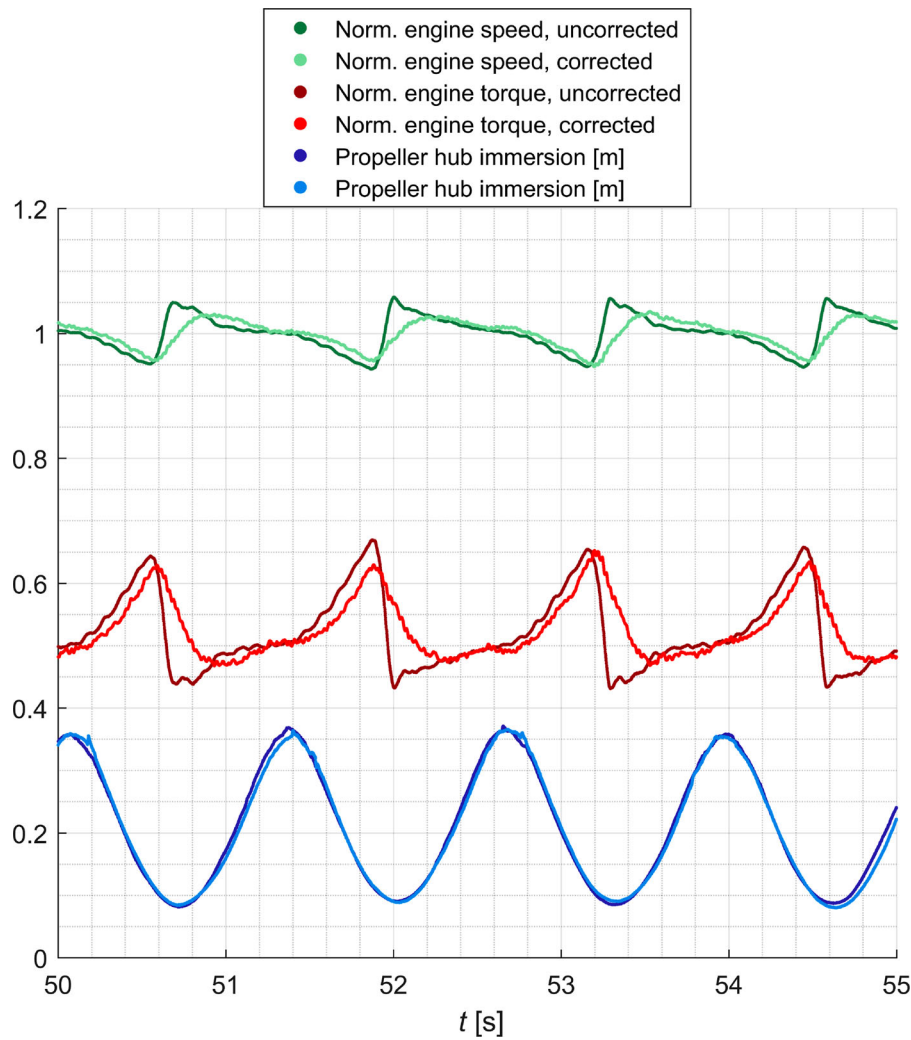


Figure 13. Time trace of engine torque and speed with emulated diesel-mechanical propulsion system, without and with numerical inertia correction. Time is expressed at model scale, with time scaled according to Froude's law. Torque and speed are normalised with respect to their nominal values. The equilibrium immersion depth of the propeller hub equals 0.218 m. The conditions during these experiments are given in Table 3. This Figure is based on the data in *exp_245.mat* (without inertia correction) and *exp_242.mat* (with inertia correction), stored in the measurement data repository (Huijgens 2020).

which is present in the drive torque, but not in the propeller load. It was demonstrated with measurements that this additional inertial component may cause a significant increase in dynamic machinery load. Failing to correct for the moment of inertia results in incorrect estimation of these dynamic loads and thus, the performance and wear of propulsion machinery at full scale. This in turn may lead to overpowered or, worse, dangerously underpowered ships. It is therefore concluded that a HIL setup with a correction for the moment of inertia is required when conducting experiments on the performance of ships in dynamic environments such as rough seas.

As was discussed earlier, the HIL experiments in this paper were conducted with an open water setup. As the term implies, this means that the propeller operates in open, undisturbed water rather than the wake field of a ship's hull. The wake field likely has a significant influence on the ventilation events. The setup discussed in this paper may therefore be mostly suited for theoretical studies on the interaction during ventilation events. For more accurate studies of ventilating propellers behind a ship's hull, different setups may be necessary. For example, free sailing model tests would include a model hull, potentially allowing more accurate reproduction of propeller ventilation as well as allowing for more realistic manoeuvring tests also in extreme condition. While a free sailing model would introduce

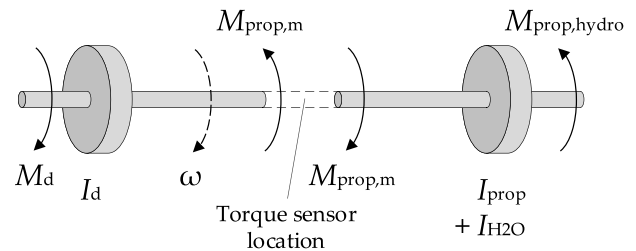


Figure 14. Schematic representation of the torque components in the (emulated) ship propulsion system. Measured propeller torque $M_{prop,m}$ includes hydrodynamic propeller load torque $M_{prop,hydro}$ and the acceleration torque components related to the inertia of the propeller, I_{prop} , and entrained water, I_{H2O} . Engine drive torque M_d contains the acceleration torque component related to the inertia of the (emulated) propulsion system, I_d , as well as the torque components present in $M_{prop,m}$. As friction losses are corrected for in the described HIL experiments, such losses are neglected here.

additional scale effects related to flow around the hull, the HIL techniques described in this paper could be as easily be applied in such experiments. The experiments presented in this paper should thus not be considered as a fully developed method to study propeller

ventilation, but rather as a demonstration that HIL provides significant added value to model basin tests. In addition, HIL open water experiments could be used to validate fully numerical models that aim to simulate the interaction between machinery and propellers in a highly dynamic environments.

Based on these conclusions, recommendations can be formulated. A first recommendation pertains the different effect of inertia on dynamic propeller performance and emulated machinery load. In the case reported in this paper, a change in moment of inertia has no significant effect on torque and thrust breakdown caused by propeller ventilation, while there is a significant effect on shaft speed and prime mover torque. Although this does not automatically apply to every propulsion system, the underlying mechanisms could be relevant for ship design and operation. Further attention to this subject is therefore recommended. From a first analysis, a hypothesis for the mechanisms behind propeller-engine interaction during ventilation events was formulated in Section 3.2. A further, more systematic analysis of this interaction is recommended for future research, with the aim of answering the following question:

How do variables such as wave encounter frequencies, wave heights, moment of inertia, equilibrium values and controller settings affect the interaction between propeller and prime mover in a dynamic environment?

Secondly, it is recommended that HIL is applied also in free-sailing model experiments when complex, non-linear dynamic interaction is expected between propulsion system and environment. For example, manoeuvring tests could be conducted in a more realistic and therefore, accurate manner if HIL were introduced. Especially in extreme environments inducing rapid load fluctuations, the introduction of HIL would bring noticeable improvements.

A third and final recommendation concerns the use of HIL to evaluate and demonstrate new technologies for ship propulsion. It is recommended that, before applying new propulsion concepts based on, for example, spark ignition engines and fuel cells, the dynamic performance of these propulsion concepts is evaluated in model basin HIL experiments. Model basin experiments shed more light on complex phenomena such as the interaction between a ventilating propeller and propulsion machinery, especially when considering phenomena occurring on small time scales. Such complex, dynamic interactions can set important limits on the safe operation of a ship. In this paper, it was demonstrated that crucial aspects related to propeller thrust and machinery load may be overlooked if HIL is not or only partly applied. It is therefore recommended that model basin HIL experiments are conducted with the corrections proposed by Huijgens et al. (2021) applied, for example adding to the validity of survivability studies with free-sailing model ships. If properly used, HIL in the ship model basin can not only contribute to a safe application of novel propulsion technologies, but also accelerate their acceptance.

Acknowledgments

The authors would like to thank the technical and scientific staff at the TU Delft model basin, and the engineers and scientists at MARIN involved in the development of the open water setup used for the described HIL experiments. In addition, the authors owe their gratitude to prof.dr. Marco Altosole and prof.dr.ir. Thomas van Terwisga for the fruitful discussions on the topics covered in this paper.

Disclosure statement

No potential conflict of interest was reported by the author(s).

Notes on contributors

Lode Huijgens, MSc and PhD in marine technology at Technische Universiteit Delft, currently works at Equinor ASA.

Arthur Vrijdag, MSc and PhD in marine technology at Technische Universiteit Delft, currently works at AVR Maritime bv.

Hans Hopman, professor ship design (maritime and transport engineering), Technische Universiteit Delft.

ORCID

Lode Huijgens  <http://orcid.org/0000-0003-0018-843X>

Arthur Vrijdag  <http://orcid.org/0000-0003-3437-2788>

Hans Hopman  <http://orcid.org/0000-0002-5404-5699>

References

- Bondarenko O, Kashiwagi M. 2010. Dynamic behavior of ship propulsion plant in actual seas. *J Jpn Inst Mar Eng.* 45:76–80. doi:10.5988/jime.45.1012
- Bondarenko O, Kashiwagi M. 2011. Statistical consideration of propeller load fluctuation at racing condition in irregular waves. *J Mar Sci Technol.* 16:402–410.
- Bondarenko O, Kitagawa Y. 2021. Development of detailed engine model for evaluation ship performance in waves by a self-propulsion model test. *J Mar Sci Technol.* 6:266–277. doi:10.1007/s00773-021-00832-y
- Burrill LC, Robson W. 1962. Virtual mass and moment of inertia of propellers. Vol. 78, Trans. North East Coast Institution of Engineers and Shipbuilders.
- Califano A. 2010. Dynamic loads on marine propellers due to intermittent ventilation. Trondheim, Norway: Norwegian University of Science and Technology.
- Califano A, Steen S. 2021. Numerical simulations of a fully submerged propeller subject to ventilation. *Ocean Eng.* 38:1582–1599. doi:10.1016/j.oceaneng.2011.07.010
- Carrica PM, Kerkvliet M, Quadvlieg FHHA, Pontarelli M, Martin JE. 2016. CFD simulations and experiments of a maneuvering generic submarine and prognosis for simulation of near surface operation. In: Proceedings of the 31st symposium on naval hydrodynamics, Monterey, USA.
- Dang J, Van-den-Boom HJJ, Ligtelijn JT. 2013. The wageningen C- and D-series propellers. In: Proceedings of the 12th international conference on fast sea transportation (FAST), Amsterdam, the Netherlands.
- Huijgens LJG. 2020. Replication data for: hardware in the loop emulation of ship propulsion systems at model scale. doi:10.34894/ORXL9Y
- Huijgens LJG. 2021. Hardware in the loop emulation of ship propulsion systems at model scale. Delft, the Netherlands: Delft University of Technology.
- Huijgens LJG, Vrijdag A, Hopman JJ. 2018. Propeller-engine interaction in a dynamic model scale environment. In: Proceedings of the 28th international ocean and polar engineering conference (ISOPE), Sapporo, Japan.
- Huijgens LJG, Vrijdag A, Hopman JJ. 2021. Hardware in the loop experiments with ship propulsion systems in the towing tank: scale effects, corrections and demonstration. *Ocean Eng.* 226. Article ID 108789. doi:10.1016/j.oceaneng.2021.108789
- ITTC. 2011. Recommended procedures and guidelines: resistance test, 7.5-02-02-01 [technical report].
- ITTC. 2014. Recommended procedures and guidelines: 1978 ITTC performance prediction method, 7.5-02-03-01.4 [technical report].
- Kitagawa Y, Bondarenko O, Tsukada Y. 2019. An experimental method to identify a component of wave orbital motion in propeller effective inflow velocity and its effects on load fluctuations of a ship main engine in waves. *Appl Ocean Res.* 92. Article ID 101922. doi:10.1016/j.apor.2019.101922
- Kitagawa Y, Bondarenko O, Tsukada Y, Fukuda T, Tanizawa K. 2018. An application of the tank test with a model ship for design of ship propulsion plant system. *Mar Eng.* 53:355–361. doi:10.5988/jime.53.355
- Kitagawa Y, Tanizawa K, Tsukada Y. 2014. Development of an experimental methodology for self-propulsion test with a marine diesel engine simulator, third report: auxiliary thruster system. In: Proceedings of the 24th international ocean and polar engineering conference (ISOPE), Busan, Korea.
- Kitagawa Y, Tanizawa K, Tsukada Y. 2015. Development of an experimental methodology for self-propulsion test with a marine diesel engine simulator, fourth report: direct measurement of actual ship speed in waves by model tests. In: Proceedings of the 25th international ocean and polar engineering conference (ISOPE), Kona, USA.
- Koushan K. 2007. Dynamics of propeller blade and duct loading on ventilated thrusters in dynamic positioning mode. In: Proceedings of the 2007 dynamic positioning conference, Houston, USA.
- Kozłowska AM, Dalheim ØØ, Savio L, Steen S. 2020. Time domain modeling of propeller forces due to ventilation in static and dynamic conditions. *J Mar Sci Eng.* 8:31. doi:10.3390/jmse8010031
- Kozłowska AM, Steen S, Koushan K. 2009. Classification of different type of propeller ventilation and ventilation inception mechanism. In: Proceedings of the first international symposium on marine propulsors (SMP'09), Trondheim, Norway.

- Krüger S, Abels W. 2017. Hydrodynamic damping and added mass of modern screw propellers. In: Proceedings of the 36th international conference on ocean and arctic engineering (OMAE), Trondheim, Norway.
- Lewis FM, Auslaender JM. 1960. Virtual inertia of propellers. *J Ship Res.* 3:37–46.
- Li J, Qu Y, Chen Y, Hua H. 2018. Investigation of added mass and damping coefficients of underwater rotating propeller using a frequency-domain panel method. *J Sound Vib.* 432:602–620. doi:10.1016/j.jsv.2018.06.060
- Martio J, Sánchez-Caja A, Siikonen T. 2015. Evaluation of propeller virtual mass and damping coefficients by URANS-method. In: Proceedings of the fourth international symposium on marine propulsors (smp'15), Austin, USA.
- Parsons MG, Vorus WS, Richard EM. 1980. Added mass and damping of vibrating propellers [technical report]. University of Michigan, Department of Naval Architecture.
- Pierson WJ, Moskowitz LA. 1964. Proposed spectral form for fully developed wind seas based on the similarity theory of S. A. Kitaigorodskii. *J Geophys Res.* 69:5181–5190.
- Sasaa K, Faltinsen OM, Lu LF, Sasaki W, Prpić-Oršić J, Kashiwagi M, Ikebuchi T. 2017. Development and validation of speed loss for a blunt-shaped ship in two rough sea voyages in the Southern Hemisphere. *Ocean Eng.* 142:577–596.
- Schwanecke H. 1963. Gedanken zur Frage der hydrodynamischen Schwingungserregung des Propellers und der Wellenleitung. In: *Jahrbuch Schiffbautechnische Gesellschaft*, p. 252–280. Berlin, Germany: Versuchsanstalt für Wasserbau und Schiffbau.
- Shigunov V, Moctar O, Papanikolaou A, Potthoff R, Liu S. 2018. International benchmark study on numerical simulation methods for prediction of manoeuvrability of ships in waves. *Ocean Eng.* 165:365–385. doi:10.1016/j.oceaneng.2018.07.031
- Shigunov V, Papanikolaou A. 2015. Criteria for minimum powering and maneuverability in adverse weather conditions. *Ship Technol Res.* 62:140–147. doi:10.1080/09377255.2015.1104090
- Smogeli Ø.N. 2006. Control of marine propellers: from normal to extreme conditions. Trondheim, Norway: Norwegian University of Science and Technology.
- Suzuki R, Tsukada Y, Ueno M. 2019. Estimation of full-scale ship manoeuvring motions from free-running model test with consideration of the operational limit of an engine. *Ocean Eng.* 172:697–711. doi:10.1016/j.oceaneng.2018.12.044
- Swales PD, Wright AJ, McGregor RC, Rothblum R. 1974. The mechanism of ventilation inception on surface piercing foils. *J Mech Eng Sci.* 16:18–24.
- Tanizawa K, Kitagawa Y, Hirata K, Fukazawa M. 2013a. Development of an experimental methodology for self-propulsion test with a marine diesel engine simulator, the second report – propeller pitch control. In: Proceedings of the 23rd international offshore and polar engineering conference (ISOPE), Anchorage, USA.
- Tanizawa K, Kitagawa Y, Takimoto T, Tsukada Y. 2013b. Development of an experimental methodology for self-propulsion test with a marine diesel engine simulator. *Int J Offshore Polar Eng.* 23:197–204.
- Ueno M, Suzuki R, Tsukada Y. 2017. Estimation of stopping ability of full-scale ship using free-running model. *Ocean Eng.* 130:260–273. doi:10.1016/j.oceaneng.2016.12.001
- Ueno M, Tsukada Y. 2015. Rudder effectiveness and speed correction for scale model ship testing. *Ocean Eng.* 109:495–506. doi:10.1016/j.oceaneng.2015.09.041
- Ueno M, Tsukada Y. 2016. Estimation of full-scale propeller torque and thrust using free-running model ship in waves. *Ocean Eng.* 120:30–39. doi:10.1016/j.oceaneng.2016.05.005
- van Biert L, Godjevac M, Visser K, Aravind PV. 2016. A review of fuel cell systems for maritime applications. *J Power Sour.* 327:345–364.
- Vrijdag A. 2016. Potential of hardware-in-the-loop simulation in the towing tank. In: Proceedings of the OCEANS 2016 MTS/IEEE conference, Monterey, USA. doi:10.1109/OCEANS.2016.7761060
- Wang G, Jia D, Cao M, Sheng Z. 1989. Propeller air ventilation and performance of ventilated propeller. In: Proceedings of the fourth international symposium on practical design of ships and mobil units (PRADS), Varna, Bulgaria.
- Zhang W, Ma N, Xiechong G, Peiyuan F. 2021. Dynamic loads and thrust hysteresis of near-surface open propeller in regular head waves—an experimental study in a circulating water channel. *Ocean Eng.* 219:1–17. doi:10.1016/j.oceaneng.2020.108359

Appendix. Nomenclature

A Notation

A	Amplitude
D	[m] Propeller diameter
g	[m/s ²] Gravity constant
h	[m] Propeller immersion
I	[kgm ²] Moment of inertia
i_{gb}	[–] Gearbox reduction ratio
M	[Nm] Torque
n	[rpm] Shaft speed
P/D	[–] Propeller pitch/diameter ratio
P	[W] Power
T	[N] Thrust
t	[s] Time
v	[m/s] Speed
λ	[–] Geometric scale factor
ω	[rad/s] Wave frequency

Subscripts

0	Equilibrium
a	Advance
b	Brake
d	Drive
E	Encounter
e	Engine
H2O	Entrained water
hydro	Hydrodynamic load
mech	Mechanical components
nom	Nominal
prop	Propeller
p	Wave peak
s	Ship
tot	Total